Absorption Characteristics of Si_3N_4 Ablation Layer Plasma

By

Hiroyuki SHIRAI*

(February 1, 1988)

Summary: The equilibrium composition and spectral absorption coefficient of Si_3N_4 ablation layer plasmas have been calculated for temperature of 3000 to 9000 K, layer thickness of 0 to 0.5cm, and pressure of 2 to 5 atm. In the calculation of radiation, molecular bands, atomic lines and continuum processes are included. These results are applied to a simple shock layer model to assess the effectiveness of the ablation layers for a blockage of high-temperature radiation from a stagnation shock layer composed of hydrogen and helium. The results show that the photoionization process of a Si atom is mainly responsible for blocking the radiation, and that the Si_3N_4 ablation layer is very effective in reducing the radiative heating due to high-energy photons.

1. INTRODUCTION

Probes entering an atmosphere of the major planets receive severe radiative heating from the environmental flow field [*1*]. Generally, ablating heat shields are employed so that an ablation layer developing along the probe surface absorbs the radiation and hence decreases the heat flux. The effectiveness of such an ablation layer is primarily determined by energy distribution of the radiation and absorption properties of the ablation layer plasma.

In the present study, the absorption characteristics of an ablation plasma generated by the ablation of a new ceramics Si_3N_4 are investigated by using a simple fluid dynamical model for a stagnation shock layer. The population density of various species in the ablation layer is obtained by the equilibrium calculation to compute the absorption coefficient of the ablation plasma. An atmosphere upstream of the shock layer is assumed to consist of 85%-hydrogen and 15%-helium by volume. The reduction of the radiative heating from the shock layer plasma by the Si_3N_4 ablation layer is investigated theoretically. The calculation is conducted mostly for the shock layer with temperature of 15,000 K and pressure of 5 atm and for the ablation layer with temperature of 6000 K. These are the typical entry conditions into the Jovian atmosphere.

2. SHOCK LAYER MODEL

A simple two-layer model shown in Fig. 1 is used to estimate the radiative heating to the stagnation point 0 from the shock layer [*2*]. The outer layer of thickness L_s is a

* Faculty of Engineering, Gunma University.

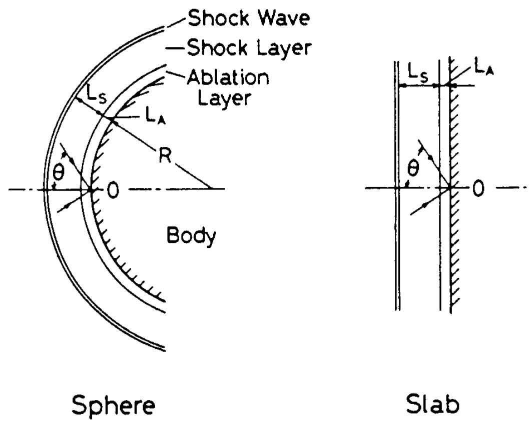

Fig. 1. Shock layer model.
(Sphere and Slab models.)

high-temperature shock layer which consists of species from the atmosphere. The inner layer of thickness L_A is an ablation layer and contains only ablation species. The body, shock layer and ablation layer are assumed to be all spherical and concentric. For this model, temperatures and densities of the two layers are different from each other, but pressures are the same and uniform.

The basic equation of the radiative energy transfer in the ablation layer is given by

$$\frac{dI_\nu}{dx}=k_\nu(I_\nu-B_\nu) \tag{1}$$

with the following boundary condition at the surface of the ablation layer

$$I_\nu=D_\nu, \tag{2}$$

where I_ν is the specific intensity at frequency ν along an optical path x, k_ν the absorption coefficient, B_ν the Planck function and $D_\nu$the radiation intensity incident on the ablation layer. The formal solution of Eqs. (1) and (2) for the optical path with an angle θ measured from the normal is

$$I_\nu=D_\nu \exp(-k_\nu l_A)+B_\nu[1-\exp(-k_\nu l_A)], \tag{3}$$

where I_ν is the radiation intensity at the stagnation point. The optical path length of the ablation layer is given by (see Fig. 1).

$$l_A=\sqrt{R^2\cos^2\theta+L_A^2+2RL_A}-R\cos\theta. \tag{4}$$

In the Eq. (3), the first term on the right hand side represents the effect of the radiative absorption by the ablation layer, and the second one means the radiative emission of the ablation layer. The radiation intensity and also the radiative absorption of the ablation plasma depend on the path length and the absorption coefficient. Therefore, in order to evaluate the effectiveness of the ablation layer, the composition and absorption coefficient of the ablation plasma must be calculated.

3. Equilibrium Composition of Ablation Plasma

The ablation and shock layer plasmas are assumed to be chemically and thermally in equilibrium independently. For the plasma conditions of interest, the following reactions must be considered in the ablation layer.

(R1) $Si_3N_4 \rightarrow 3Si + 2N_2$	(R2) $Si(l) \rightleftharpoons Si(g)$
(R3) $2Si \rightleftharpoons Si_2$	(R4) $Si \rightleftharpoons Si^+ + e$
(R5) $N_2 \rightleftharpoons 2N$	(R6) $N_2 \rightleftharpoons N_2^+ + e$
(R7) $N \rightleftharpoons N^+ + e$	(R8) $Si + N \rightleftharpoons SiN$

The first reaction (R1) represents the decomposition of solid Si_3N_4, and the second one (R2) gasifying reaction of liquid silicon. The others are all gas-phase reactions. The equilibrium constants for the reactions (R2), (R3), (R5) and (R8) are taken from JANAF thermochemical table[(3)], and those for the reactions (R4), (R6) and (R7) are given by the usual Saha equilibrium relation.

An example of the equilibrium composition of the ablation plasma is shown in Fig. 2. The abscissa represents the ablation layer temperature and the ordinate indicates the number densities of the ablation species. It is noted from the figure that for the condition treated, Si atoms and N_2 molecules are predominant. In the high-temperature region, the concentration of N atoms is increased.

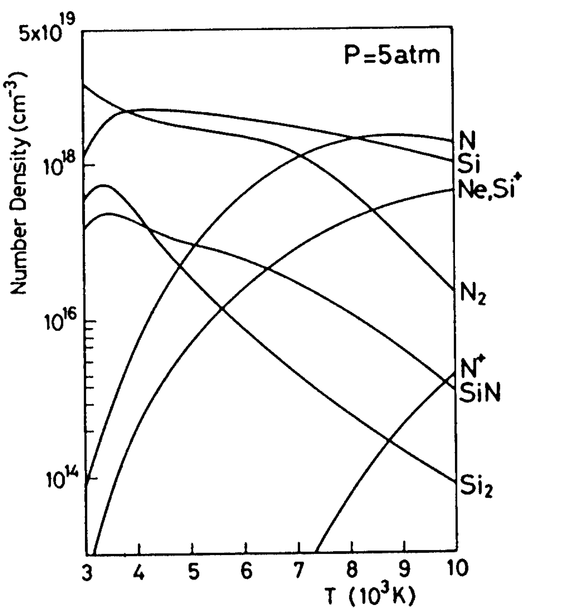

Fig. 2. Equilibrium composition of Si_3N_4 plasma.

4. Calculation of Absorption Coefficient of Ablation Plasma

From the above result of the equilibrium composition, the radiative absorptions due to N_2 molecules, Si and N atoms are taken into consideration as follows: [1] First positive (1P) band of N_2, [2] second positive (2P) band of N_2, [3] Vegard-Kaplan (VK) band of N_2, [4] Lyman-Birge-Hopfield (LBH) band of N_2, [5] Birge-Hopfield (BH) band of N_2, [6] bound-bound (b-b), bound-free (b-f), free-free (f-f) transitions for N atoms, and [7] b-b, b-f, f-f transitions for Si atoms.

Molecular absorption coefficients were approximately calculated by the smeared rotational line model [4]. The vibrational levels taken into consideration in the present study are as follows (v′=upper vibrational quantum number and v″=lower one):v′=0−8 and v″=0−9 for the 1P band, v′=0−4 and v″=0−10 for the 2P band, v′=0−8 and v″=0−10 for the VK band, and v′=0−6 and v″=0−10 for the LBH band. For the N_2 BH band, an approximate absorption coefficient is adopted from Hoshizaki and Wilson [5]. To calculate the molecular absorption coefficients, basic physical quantities such as rotational and vibrational constants, and Franck-Condon factors are necessary. These are taken from literatures [6] [7].

For an atomic b-b transition from a lower electronic level l to an upper level u, the absorption cross section and the absorption coefficient can be written as

$$\sigma_{lu}(\nu)=\frac{\pi e^2}{m_a c} f_{lu} b_{lu}(\nu) \tag{5}$$

$$k_\nu^{bb}=N_l\sigma_{lu}(\nu)=\frac{g_l}{Q}N\sigma_{lu}(\nu)\exp\left(-E_l/kT_A\right), \tag{6}$$

where m_a is the mass of an atom, c the velocity of light, f_{lu} the f-number for the transition, $b_{lu}(\nu)$ the shape of the line, N_l the number density at the lower level, g_l the statistical weight of the same level, E_l the electronic excitation energy, Q the electronic partition function, T_A the temperature of an ablation layer, and k the Boltzmann constant. Generally, for the plasma conditions of interest, the important line broadening mechanism is electronic Stark broadening and Doppler broadening. Therefore, the lines acquire a Voigt shape, whose simplified expression is given in Ref. 8. The absorption coefficient decreases rapidly with increasing E_l.

The 57 nitrogen lines with the wavelength of 85.29 to 174.3 nm whose lower level is ^{4}S(E_l=0, ground level), ^{2}D(E_l=2.383 eV) or ^{2}P(E_l=3.576 eV) are included in the calculations. The data of f-number, E_l, g_l, wavelength and half-width of Stark broadening for these lines are given by Wilson and Nicolet [9]. For Si atoms, the most important 25 lines are selected from Wiese's data [10]. Stark broadening data for these lines are taken from Ref. 11.

The absorption coefficients for the atomic nitrogen b-f and f-f transitions have been calculated for wide conditions of temperature and photon energy by Wilson and Nicolet [9]. Those for Si atoms are calculated according to the method of Biberman and Norman [12]. The absorption cross section for the Si b-f transition is adopted from Barfield's data [13].

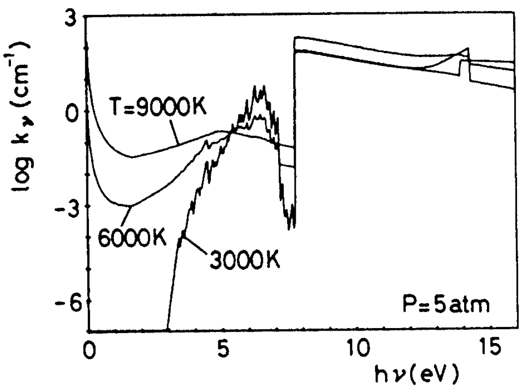

Fig. 3. Distributions of absorption coefficient at T_A=3000, 6000 and 9000 K.

The total absorption coefficient at any frequency ν is the sum of all the contributions mentioned above. Therefore, it can be easily calculated for a required spectral range. Figure 3 shows the distributions of the absorption coefficient thus calculated at T_A=3000, 6000 and 9000 K for pressure of P=5 atm. Below $h\nu$=7.8 eV, the molecular nitrogen bands and atomic f-f transition are responsible for the value of k_ν. For the energy range of $h\nu$>7.8 eV, the absorption by the Si b-f transition (photoionization) is predominant. The absorption due to the atomic b-b transitions is unimportant for those conditions.

5. Calculation of Radiative Heat Flux from Shock Layer

It is possible to calculate the equilibrium compostion of the shock layer plasma with high accuracy.(14) For the shock layer under consideration, inclusion only of H, H^+, He and e is sufficient. Their number densities for the conditions with temperature of 15,000 K and pressure of 5 atm are n_H=1.421×10^{18} cm^{-3}, n_{He}=1.634×10^{17}, and $n_H{}^+=n_e$=4.311×10^{17} cm^{-3}. For this equilibrium composition, the H b-b line radiation, f-b continuum radiation due to H^+-e recombination, and f-f bremsstrahlung are taken into account as a shock layer radiation. The contribution of He is negligibly small.

The expression for the total energy (per unit volume and per unit solid angle) of the spontaneous emission of a single line is

$$E=\frac{h_\nu A_{ul}}{4\pi}\frac{Ng_u}{Q}\exp\left(-E_u/kT_s\right), \tag{7}$$

where A_{ul} is the radiative transition probability, N the number density of an atom, g_u the statiatical weight of an upper level, E_u the upper-level electronic excitation energy, Q the partition function, and T_s the shock layer temperature. If the shape of the line is expressed by $b_{ul}(\nu)$, the radiative energy at ν due to the spectral line becomes $Eb_{ul}(\nu)$. Therefore, the absorption coefficient at the same frequency is given by

$$k_\nu^{bb}=Eb_{ul}(\nu)/B_\nu. \tag{8}$$

The calculations included 14 atomic hydrogen lines: the Lyman L_α (centered at 121.57 nm), L_β (102.57 nm), L_γ (97.25 nm), L_δ (94.97 nm); the Balmer H_α (656.28 nm), H_β (486.13 nm), H_γ (434.05 nm), H_δ (410.17 nm); the Paschen P_α (1875.1 nm), P_β (1281.81 nm), P_γ (1093.81 nm); as well as three lines at 4051.2, 2625.2 and 7457.8 nm. The radiative transition probability, electronic excitation energy and statistical weight for these lines are well known and are taken from Ref. 10. The shape of the Lyman and Balmer lines is calculated by using the detailed tables of Vidal et al [*15*]. The remaining H lines are assumed to be governed by the Stark Broadening and their widths are calculated according to the method of Lasher et al [*16*].

The absorption coefficient at ν due to the continuous f-b and f-f transitions of atomic hydrogen is given by [*17*]

$$k_\nu^c=\frac{16}{3}\left(\frac{\pi}{6m^3}\right)^{1/2}\frac{e^6}{2hc\nu^3}\frac{n_e n_i}{(kT_s)^{1/2}} \times\left[1-\exp\left(-\frac{h\nu}{kT_s}\right)\right]\left[\frac{2E_H}{kT_s}\exp\left(-\frac{\Delta E_H}{kT_s}\right)\sum\frac{\gamma_{fb}}{n^3}\exp\left(\frac{E_H}{n^2kT}\right)+\gamma_{ff}\right], \tag{9}$$

where E_H is the ionization potential of a hydrogen atom, ΔE_H the lowering of the ionization potential, n the principal quantum number of an electronic energy level, n_i the number density of a H^+ ion, and γ_{fb} and γ_{ff} are the Gaunt factors for the b-f and f-f transitions, respectively. These Gaunt factors are taken from Karzas and Latter [*18*]. ΔE_H is calculated by the method of Ref. 19. The continua for $n\leq6$ are included in the calculations because the levels with $n\geq7$ merge into the continuum under the plasma conditions of interest [*20*].

The total absorption coefficient k_ν^H is the sum of all these constituents. Then, D_ν in Eq. (3) becomes

$$D_\nu=B_\nu[1-\exp(-k_\nu^H l_S)], \tag{10}$$

where the optical path length of the shock layer is given by

$$l_S=\sqrt{R^2\cos^2\theta+(L_A+L_S)^2+2R(L_A+L_S)}-R\cos\theta-l_A. \tag{11}$$

Figure 4 shows the energy distribution of the radiation falling at an angle of θ=45 on the stagnation point from the shock layer plasma. The calculations were conducted for the following conditions: T_s=15,000 K, P=5 atm, R=35 cm, L_S=2.5 cm, and L_A=0 and 0.5 cm. The radiation above $h\nu$=7.8 eV is completely absorbed by the Si photoionization process. Around $h\nu$=5 eV, the absorption by the N_2 VK band is expected to some extent, but the remaining bands hardly contribute to the absorption. Such a situation is substantially unchanged for other values of T_A and θ.

The same calculations were made for T_S=20,000 K, P=2 atm and T_A=5000 K, and the result is shown in Fig. 5. Comparing it with Fig. 4, one can see that the radiation in the high energy region is very important and it is also absorbed very effectively by the

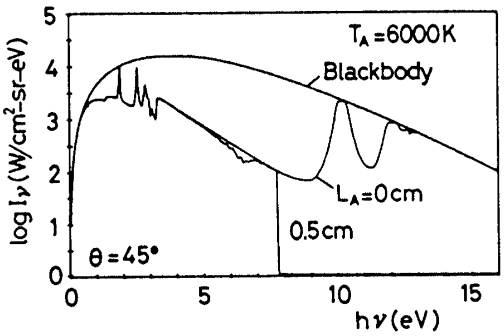

Fig. 4. Spectral distribution of radiative intensity from the shock layer.
(T_S=15,000 K, T_A=6000 K and P=5 atm.)

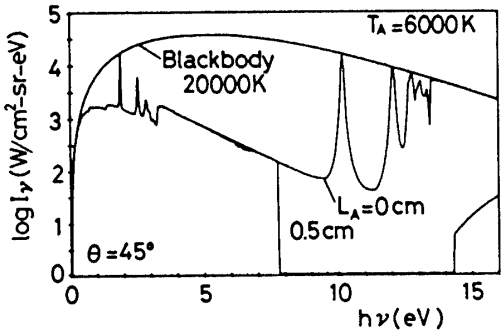

Fig. 5. Spectral distribution of radiative intensity from the shock layer.
(T_S=20,000 K, T_A=6000 K and P=2 atm.)

Si_3N_4 ablation layer. The both figures show clearly that the Si photoionization is the major process responsible for reducing the radiation reaching the stagnation point.

The total radiative heat flux to the stagnation point 0 in Fig. 1 is expressed as

$$q=\pi \int_0^{\pi/2} \left(\int_0^{\infty} I_\nu d\nu\right) \sin 2\theta d\theta. \tag{12}$$

Figure 6 shows the angular distribution of the radiative heat flux at T_A=6000 K as a function of θ for two values of the ablation layer thickness. The plasma conditions in Figs. 6(a) and (b) coresspond to those in Fig. 5 and Fig. 4, respectively. In the both figures, the results for the slab approximation are also shown by the broken lines. This approximation overestimates the optical path length of the off-axis rays. This causes overestimation of the contribution of those rays to the overall radiative transport.

Table 1 contains the absorption rate of the Si_3N_4 ablation layer for several plasma conditions. For example, in the case of the condition ①, the radiative heat flux reaches 44.5 kW/cm^2 if there is no ablation layer, but the ablation layer with thickness of L_A=0.25 cm reduces it to 34.3 kW. It is apparent that the thickness of the ablation layer is not a critical parameter for the Si_3N_4 ablation layer. It is possible to conclude that the ablation layer is very effective for the condition in which the high-energy photons play an important role.

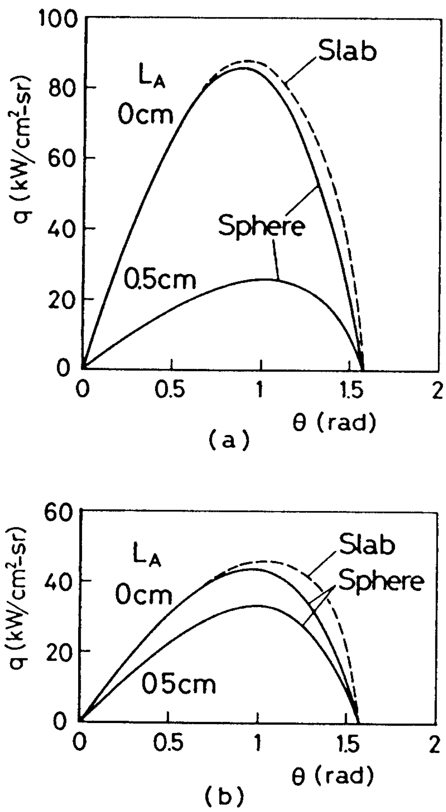

Fig. 6. Angular distribution of radiative heat-transfer rate for the stagnation point.
(upper: T_S=20,000 K, T_A=6000 K and P=2 atm. lower: T_S=20,000 K, T_A=6000 K and P=5 atm.)

Table 1. Absorption rate for several plasma conditions

	①	②	③	④
Shock Layer				
T(K)	15000	15000	15000	20000
P(atm)	5	5	5	2
Thickness (cm)	2.5	2.5	2.5	2.5
Ablation Layer				
T(K)	6000	6000	3000	6000
Thickness (cm)	0.25	0.5	0.5	0.5
No Ablation (W/cm^2)	44.5	44.5	44.5	88.2
Ablation (W/cm^2)	34.3	33.5	33.4	26.3
Absorption (%)	22.9	24.7	24.9	70.2

6. Conclusions

Using the much simplified shock layer model, the absorption coefficient of the Si_3N_4 ablation plasma was calculated for the equilibrium plasma compositions. In order to evaluate the effectiveness of the ablation layer, the reduction of the radiative heat flux from the shock layer plasma composed of hydrogen and helium was investigated numerically. The main conclutions are as follows.

(1) The Si_3N_4 ablation layer is very effective in blocking the radiative heating due to high-energy photons from the shock layer.

(2) The Si photoionization process is mainly responsible for reducing the radiation. The absorption due to the atomic b-b transitions is very small.

(3) The N_2 molecular bands are not expected to contribute much to the absorption.

References

[1] For example, Moss, J. N.: Entry Heating and Thermal Protection, Prog. Astronaut. Aeronaut., Vol. 69 (1980), p. 3.
[2] Nelson, H. F.: J. Quant. Spectrosc. Radiat. Transf., Vol. 13 (1973), p. 427.
[3] JANAF, Thermochemical Table, (1965).
[4] Penner, S. S. and Olfe, D. B.: Radiation and Reentry, (1968), p. 23, Academic Press.
[5] Hoshizaki, H. and Wilson, K. H.: AIAA J., Vol. 5, No. 1, (1967), p. 25.
[6] Herzberg, G.: Molecular Spectra and Molecular Structure, I. Spectra of Diatomic Molecules, (1950), p. 551, Van Nostrand Reinhold Co.
[7] Suchard, S. N. and Melzer, J. E., Spectroscopic Data, Vol. 2 (1976), p. 382, IFI/Plenum.
[8] Whiting, E. E.: J. Quant. Spectrosc. Radiat. Transf., Vol. 8 (1968), p. 1379.
[9] Wilson, K. H. and Nicolet, W. E.: J. Quant. Spectrosc. Radiat. Transf., Vol. 7 (1967), p. 891.
[10] Wiese, W. L. *et al.*: Atomic Transition Probabilities, Vol. 1 (1966), p. 71, NSRDS-NBS4.
[11] Griem, H. R.: Spectral Line Broadening by Plasmas, (1974), p. 343, Academic Press.
[12] Biberman, L. M. and Norman, G. E.: J. Quant. Spectrosc. Radiat. Transf., Vol. 3 (1963), p. 221.
[13] Barfield, W. D. *et al.*: J. Quant. Spectrosc. Radiat. Transf., Vol. 12 (1972), p. 1409.
[14] Patch, R. W.: J. Quant. Spectrosc. Radiat. Transf., Vol. 9 (1969). p. 63.
[15] Vidal, C. R. *et al.*: Astrophys. J. Suppl. 214, Vol. 25 (1973), p. 37.
[16] Lasher, L. E. *et al.*: Ibid. [9], p. 305.
[17] Roberts, J. R. and Voigt, P. A.: J. Res. NBS-A., Vol. 75A (1971), p. 291.
[18] Karzas, W. J. and Latter, R.: Astrophys, J. Suppl. 55, Vol. 11 (1961), p. 167.
[19] Capitelli, M. and Molinari, E.: J. Plasma Phys., Vol. 4, No. 2 (1970), p. 335.
[20] Inglis, D. R. and Teller, E., Astrophys. J., Vol. 90 (1939), p. 439.